Fizika Nizkikh Temperatur, 1998, v. 24, No 6, p. 507–521

Thirty years ago L. I. Amstutz, J. R. Thompson, and H. Meyer detected quantum diffusion in solid hydrogen. This discovery has considerably influenced the evolution of the concept of tunnel processes in solids and stimulated numerous experimental and theoretical studies. Many aspects of this interesting phenomenon are not yet clear and its further investigation will undoubtedly reward researchers efforts with results of fundamental importance. Prof. H. Meyer, F. London Prize winner, agreed to contribute to the celebration of the anniversary and to write a paper for our Journal describing the progress achieved in quantum diffusion in solid hydrogens during the recent decade. Prof. H. Meyer is not only one of the authors of the discovery. It is to his futher studies that we owe the first experimental detection and investigation of the most interesting features of quantum diffusion in hydrogen.

Editorial Board

Quantum diffusion and tunneling in the solid hydrogens: a short review

Horst Meyer

Department of Physics, Duke University Durham, NC 27708-0305 U.S.A.
E-mail: hm@phy.duke.edu

Received December 15, 1997

The first observations 30 years ago of molecular clustering via quantum diffusion in solid H_2 in nuclear magnetic resonance (NMR) and pressure experiments are described. A previous review on quantum diffusion and tunneling up to 1986 is updated to reflect progress in the last ten years. In particular I review the effect of clustering on heat capacity in solid D_2 and on the thermal conductivity in solid H_2 . The configurational relaxation time observed in D_2 at 1.75 K is found to scale with that in H_2 at the same temperature in terms of the predictions of ortho–para resonant conversion-induced hopping. The relaxation times measured simultaneously on the same sample in NMR and conductivity experiments reflect different configurational processes. The theory of molecular hopping and pairing in solid H_2 is outlined and compared with experiments. The tunneling frequency of HD in solid H_2 deduced from transverse and longitudinal NMR relaxation experiments between 0.03 and 14 K is discussed. The hopping of ortho-H_2 , invoked as a mechanism in the enhanced ortho–para conversion in presence of O_2 impurities, is mentioned. Finally, recent tunneling results for H, D and H_2^- anions in solid H_2 during the studies of low temperature reaction dynamics are also briefly described. In the Appendix, the hopping frequency determination in HD from NMR transverse relaxation time measurements is reviewed.

PACS: **67.80.–s**

1. Introduction

It is an honor for me to have been invited by Prof. V. G. Manzhelii to write an article for the 30th anniversary of the first observation of ortho-H_2 impurity quantum diffusion in a solid para-H_2 matrix. I would like to start this article with a few reminiscences on how this phenomenon was observed. A previous review [1] has given an account of work done until fall 1986 that, besides quantum diffusion in solid hydrogen, includes tunneling of HD impurities in hcp H_2 and recombination of H in H_2 via tunneling. Since that time further progress — both theoretical and experimental — has been made in this field and there has been increased awareness of the interesting tunneling reactions as a new type of low temperature chemical reaction.

The publication of the earlier review article permits restricting the description of experiments and theory since 1986, and one of the purposes of this review is to draw attention to some of the open questions that need to be addressed. I may be forgiven for including some details and figures of yet unpublished experiments at Duke University, and also for comparing the '81 HD tunneling results with more recent ones obtained by the group of N. Sullivan.

This article is organized as follows. Sections 2 A and 2 B contain an account of the initial observation of quantum diffusion in solid H_2 , followed by experiments since 1986, — both in H_2 and in D_2 — and by the theoretical treatment of the hopping process in solid H_2 . Section 2 C deals with HD tunneling in solid H_2 including mechanisms ranging from quantum to classical diffusion. In Section 2 D, atom tunneling in both H_2 , D_2 and in their mixtures is briefly reviewed. In the Appendix, the analysis of NMR T_2 measurements to obtain the HD hopping frequency is reviewed.

2. Quantum diffusion and tunneling in solid H_2 and D_2

A. The initial observation of o-H_2 clustering in solid H_2

The observation of molecular motion in solid H_2 below 4 K was not the result of a systematic search, but was a fortunate accident brought about by a puzzling problem during NMR experiments. L.I. Amstutz, J.R. Thompson, and I were engaged in studying the NMR spectrum of ortho-H_2 impurities in a hcp matrix of para-H_2 . Ortho-H_2 has a nuclear spin $I = 1$ and a rotational angular momentum $J = 1$ and gives a proton NMR signal, while para-H_2 has $I = 0$ and $J = 0$, with no NMR signal. [Henceforth, in order to avoid confusion farther in this review, I use $(J = 1)$ and $(J = 0)$ to denote respectively ortho- and para-H_2 .] We were trying to improve recent experiments [2] where the NMR «pair spectrum» of nearest $(J = 1)H_2$ neighbors had been studied as a function of temperature, which led to the first determination of the electric quadrupole-quadrupole interaction energy parameter in solid H_2 , $\Gamma/k_B = 0.82$ K, a value that has stood the test of time.

We were studying the NMR spectrum of a sample with ortho molefraction $X(J = 1) = 0.01$, which shows two signal components: a) a sharp intense line at the Larmor frequency ν_L that represents the signal of the «isolated» $(J = 1)H_2$ molecules surrounded by 12 $(J = 1)H_2$ nearest neighbors and b) a structure with three peaks, placed symmetrically on each side of the sharp line. The center of gravity of this structure is located at a frequency $\nu(T) = \nu_L \pm \delta\nu(T)$ where $\delta\nu(T)$ increases from ≈ 0 to 20 kHz as T decreases from 4 to 0.4 K. A representative spectrum for $X = 0.06$ is shown in Fig. 1. The structure represents the «pair spectrum» of nearest $(J = 1)H_2$ neighbors and the temperature dependence of $\delta\nu$ reflects the orientational ordering

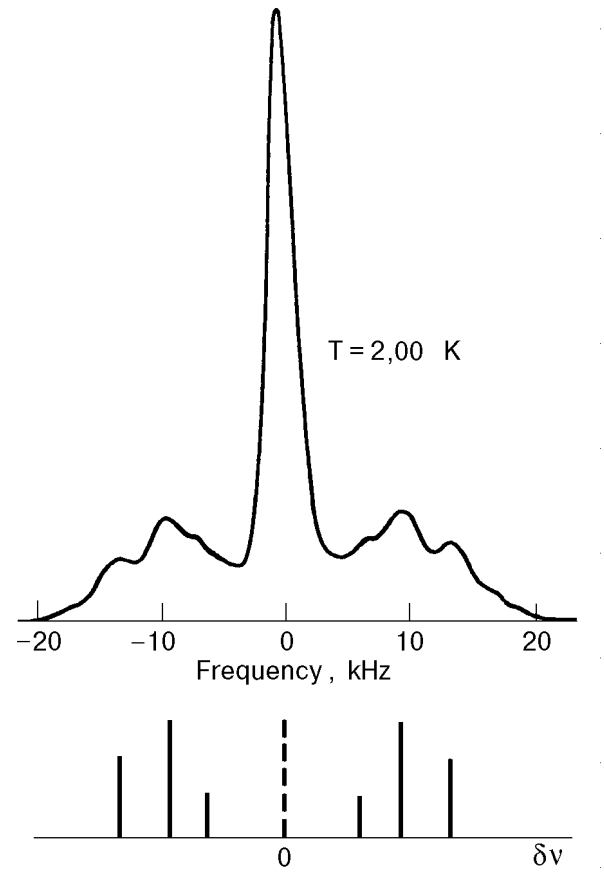

Fig. 1. Representative NMR absorption spectrum of H_2 at $X(J=1) = 0.06$ and $T = 2$ K. The spectrum under the curve represents the three pairs of satellites with their predicted respective intensities [2]. At $X(J = 1) = 0.005$, the satellite intensities are ten times smaller than in this Figure.

h a low value of $X = 0.01$, the signal of the pairs was weak at the initial temperature of our measurement $T_i \approx 2$ K and our attention was focussed on the NMR center line. We fully expected that when we decreased T, the integrated amplitude of this line should increase, because it is proportional to the nuclear susceptibility χ, which in turn is expected to obey Curie's law $\chi \propto T^{-1}$. We found indeed that, after rapidly cooling the sample by about $\Delta T \approx 0.5$ K, the signal amplitude rapidly increased, as expected. But then, to our surprise, it passed over a maximum and decreased to an equilibrium value over the course of several hours. When we warmed the sample back to T_i , the amplitude rapidly decreased at first, then increased slowly back to the original value we had at the beginning of the experiment. We first suspected that these observations resulted from a drift in the amplifier of our NMR detection equipment, and we spent much time checking and calibrating carefully our electronics. However both our Robinson spectrometer [3] and the phase-detection amplifier system

were found to perform without any drift in time. We then started to investigate this anomalous NMR signal behavior systematically and concluded that for unknown reasons over the range from 3 to 0.4 K the number of isolated o-H_2 decreased with temperature and equilibrated with a characteristic time $\tau(T)$. That time τ increased with decreasing T. Conversely, as T was increased, these isolated $(J = 1)H_2$ reappeared, as evidenced by the recovery of the signal amplitude. We wondered how this process could take place, as we knew that classical activated diffusion rate was negligible at these temperatures, because the energy barrier for vacancy hopping is ≈ 200 K in solid H_2 . We concluded that there had to be some other tunneling mechanism or molecular interchange with a rate that was not strongly temperature dependent. From previous work [2], we realized that the internal energy of isolated $(J = 1)H_2$ pairs was lower than that of the isolated $(J = 1)H_2$ «singles», and it suddenly occured to us that what we had witnessed was the clustering of $(J = 1)H_2$ into pairs as the temperature decreased, and their unclustering as the sample was warmed up. The next step in our analysis was then to form the free energy F of the total system of $(J = 1)H_2$ in the solid matrix, including both «singles», N_s , and those molecules forming nearest neighbor $(J = 1)$ «pairs», N_p , with respective fractions N_s/N and N_p/N, where N is the total number of $(J = 1)H_2$ particles. By minimizing this free energy, it was possible to calculate the equilibrium fraction of these two types at a given $X(J = 1)$ and T. The transient of the signal increase (or decrease) with time was found to be represented by an exponential $\exp(-t/\tau)$. The experimental results for the relaxation time as a function of temperature, but without a numerical calculation of the equilibrium fractions N_s/N as a function of T, were presented in our original publication [4].

But we believed that a quantitative measurement of N_s/N from NMR experiments would be affected by systematic uncertainties from electronics, geometry etc. Therefore another approach was explored: while the NMR experiments were still in progress, pressure measurements at constant volume with a sensitive strain gauge were carried out in another cryostat by Ramm and myself on samples of H_2 with similar low $(J = 1)$ concentration. We expected that after cooling the sample to a final temperature, T_{fin} , the pressure $P = (\partial F/\partial V)_T$ was going to change with time at T_{fin} while the free energy F tended to its minimum value. The change $\Delta P(T) = [P(4.2\text{ K}) - P(T_{\text{fin}})]$ to be observed between the initial temperature (4.2 K) and T_{fin} , could then be compared with calculations from simple statistical mechanics. This expectation was indeed fulfilled and the relaxation time for the equilibration process at each temperature could be obtained by automatically recording the pressure versus time. The transient $[P(t) - P(t = \infty)]$ at the temperature T_{fin} was found to follow again an exponential with the relaxation time τ. As the molecules cluster, the pressure is predicted to decrease, reflecting a more ordered orientational state in the system, and this was verified by the experiment. Just as in NMR experiments, the characteristic time to cluster upon cooling increased as T_{fin} was decreased. These experiments and their analysis were first presented in preliminary form in the thesis of Ramm [5] and a statistical analysis was also published [6] where the equilibrium concentration of «singles», «pairs», and «triangles» of $(J = 1)H_2$ and the pressure changes were calculated. The energy levels of the triangular configurations used here had been calculated by Miyagi, and independently by Harris [7].

Within a few years, optical experiments in other laboratories confirmed and measured the effects from clustering in H_2 [8–10]. The insight stimulating these experiments was provided by the important paper by Oyarzun and van Kranendonk [11] who identified the mechanism of molecular motion as the «resonant ortho–para conversion», a mechanism distinct from tunneling, and by which a $(J = 1)$ particle excitation can propagate through a lattice of $(J = 0)H_2$ molecules, leading to «quantum diffusion». The authors calculated that this mechanism was faster than that of quantum mechanical tunneling.

The final publication of Ramm's experiments was delayed by more than ten years by other seemingly higher priorities, but in hindsight for no good reasons at all. The pressure results were finally published [12] together with more recent clustering experiments [13] showing quite novel results at temperatures as low as 0.02 K, and which revived greatly the interest in this topic.

B. Research on H_2 *and* D_2 *since 1986*

1. Calorimetry. Detailed investigations of molecular clustering in the hydrogens were carried out at the B. Verkin Institute for Low Temperature Physics and Engineering in Kharkov by calorimetric methods that follow the ealier detailed studies [14]. A very interesting result was the unambiguous demonstration of $(J = 1)D_2$ clustering in a matrix of $(J = 0)D_2$, called respectively «para» and «ortho». As van Kranendonk [15] has pointed out, the mo-

lecular hopping frequency ν via resonant ortho–para conversion is $\nu \propto \gamma^2/R_0^5$, where γ is the nuclear gyromagnetic factor and R_0 is the intermolecular spacing with $R_0(H_2)/R_0(D_2) = 1.05$. The ratio for the deuteron and proton factors is $\gamma(D)/\gamma(H) = 0.154$, and hence the hopping frequency in D_2 is much smaller than in H_2. A calculation on p. 266 of Ref. 15, and which included other factors than γ, gives

$$\nu(D_2) = 0.48 \cdot 10^{-2} \nu(H_2) \ . \qquad (1)$$

To detect the effect of clustering in D_2, Bagatskii et al. [16] measured the specific heat C_p of a sample with $X(J = 1) = 0.028$ as a function of time. Two processes contribute to a slow variation of C_p with time: a) the irreversible $(J = 1) \rightarrow (J = 0)$ conversion rate that causes C_p to decrease and b) the clustering with a characteristic time τ of the isolated $J = 1$ particles into pairs via resonant $(J = 1) \leftrightarrow (J = 0)$ conversion, leading to an increase of C_p. Hence these two processes tend to compensate each other, but the good measuring accuracy enabled the authors to isolate the two contributions in the following way: the experiment started with the sample having random distribution of the p-D_2, which is reached after cooling the crystallized sample from the melting point at 18.7 K. As shown in Fig. 2, C_p slowly decreases with time during which t

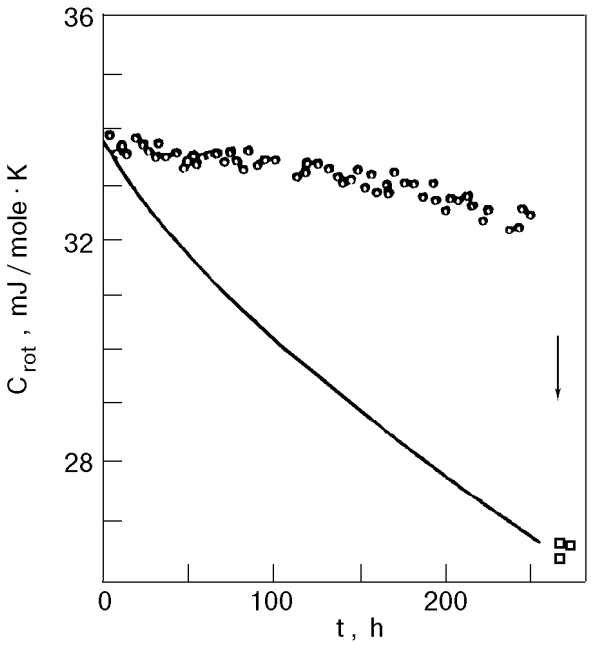

Fig. 2. Time dependence of the heat capacity C of D_2 [$X(J = 1) = 0.028$, $T = 1.73$ K]. Open circles: experimental values. Open squares: experimental data obtained after melting and recrystallizing the sample. The solid line represents the theoretical curve calculated on the assumption that no diffusion occurs ($\tau = \infty$) [16].

ed at the same temperature over a period of 250 h. The sample was then heated to the melting point and cooled back to 1.65 K over a time of about 2 h. During this time, the distribution of $(J = 1)D_2$ became randomized again, just as it was initially at the beginning of the experiment. However the mole fraction $X(J = 1)$ had decreased by conversion, and the C_p, measured again at 1.65 K, was considerably lower than before this thermal cycling operation. This decrease of C_p from the value at $t = 0$ was then due solely to conversion. From the combined analysis of the two experiments, the authors deduced a clustering characteristic time $\tau(D_2) = 630 \pm 50$ h at $T = 1.65$ K.

Comparing this result with predictions is difficult: although theory provides an estimate of the resonant conversion frequency, the predictions of the average number of hops per particle to achieve clustering is uncertain, and will be discussed in a later section. However a more immediate check of the predictions can be made by comparing the clustering time in D_2 and in H_2 under similar conditions of $X(J = 1)$ and T. Because the anisotropic electrostatic interactions, characterized by the parameter Γ, are comparable for H_2 and D_2 [$\Gamma(H_2)/\Gamma(D_2) \sim 0.8$], we can expect that the number of hops to achieve clustering is also comparable, while the ratio of the hopping rates is given by Eq. (1). From pressure measurements in H_2 at $T = 1.7$ K and with $X = 0.025$, $\tau(H_2) = 3.0$ h [12]. The ratio $\tau(H_2)/\tau(D_2) = 0.46 \cdot 10^{-2}$ is then in surprisingly good agreement with the predictions given by Eq. (1). (This scaling of the hopping times is only valid at «high» temperatures, i.e., above ≈ 0.5 K, but should not work at low temperatures where the hopping probability is more sensitive to the electric potential distortion in the surroundings and to its gradient. There the directions for a most probable jump for D_2 and for H_2 under similar conditions could be quite different, resulting in clustering trajectories of different lengths [17]. See also Section 2 B3.)

Another interesting aspect in the calorimetric studies is the effect of heavier impurities on the clustering time constant τ in solid H_2. Minchina et al. [18] reported that at two temperatures, 0.5 and 1.3 K, where the experiments were carried out, the introduction of D_2 impurities first decreases τ from the value of pure H_2. Beyond a concentration $X(D_2) = 0.02$, τ monotonically increases for doping up to $X(D_2) = 0.3$, but by less than a factor of 2 [18]. Experiments were subsequently carried out on H_2 doped with the heavier impurity neon [19]. Mixtures with $X(Ne) < 6 \cdot 10^{-4}$ showed a decrease of

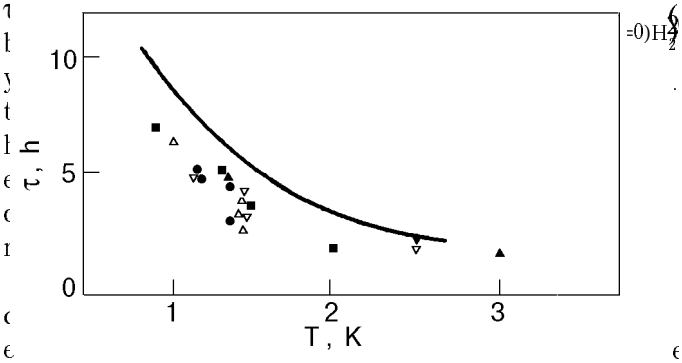

Fig. 3. Experimental values of the configurational relaxation time τ versus T in solid H_2 with added Ne impurities having a concentration n(Ne). Open triangles: n(Ne) = 0.02%, $X(J = 1)$ = = 0.5%. Inverse open triangles: n(Ne) = 0.04%, $X(J = 1) = 0.5$%. Solid circles: n(Ne) = 0.06%, $X(J = 1) = 0.5$%. Solid triangles: n(Ne) = 0.06%, $X(J = 1) = 1$%. Solid squares: H_2 with $X(J = 1)$ = = 0.5% and added impurity of 2% D_2 . The solid curve represents averaged values of τ for pure H_2 [19].

nsistent with the result for D_2 impurity doping. These results are shown in Fig. 3. The reasons for this intriguing phenomenon have been discussed in Ref. 19 in terms of lattice distortions by the heavy impurity, but this needs to be further clarified. According to Fig. 3, τ is independent of X(Ne) in the 0.02-0.06% range. It has been assumed in Ref. 19 that the upper limit of solubility of Ne in H_2 is not higher than 0.02%.

A further calorimetric experiment by the same group probed whether quantum diffusion of $(J = 1)D_2$ in $(J = 0)H_2$ could be observed [20]. A sample with 3% D_2 , corresponding to $X(J = 1) = 9.4 \cdot 10^{-4}$ of $(J = 1)D_2$ in $(J = 0)H_2$ was investigated. No evidence of a clustering on the specific heat after a period of 290 h at 1.7 K could be found, indicating the characteristing clustering time to be in excess of 10^4 h.

2. Thermal conductivity. Simultaneous thermal conductivity and NMR experiments at Duke University were carried out on a sample of solid H_2 grown at constant density, corresponding to a pressure of ≈ 90 bar, and from which information of the clustering could be obtained [21]. More recently, further conductivity experiments [22] at a similar pressure were carried out in another cell where the sample was grown at constant pressure [23] instead of constant volume. Such a check with a different crystal growth arrangement was made necessary in view of the unusual results reported in Ref. 21. To analyze the results, the additivity of the thermal resistivities from phonon scattering is assumed, namely

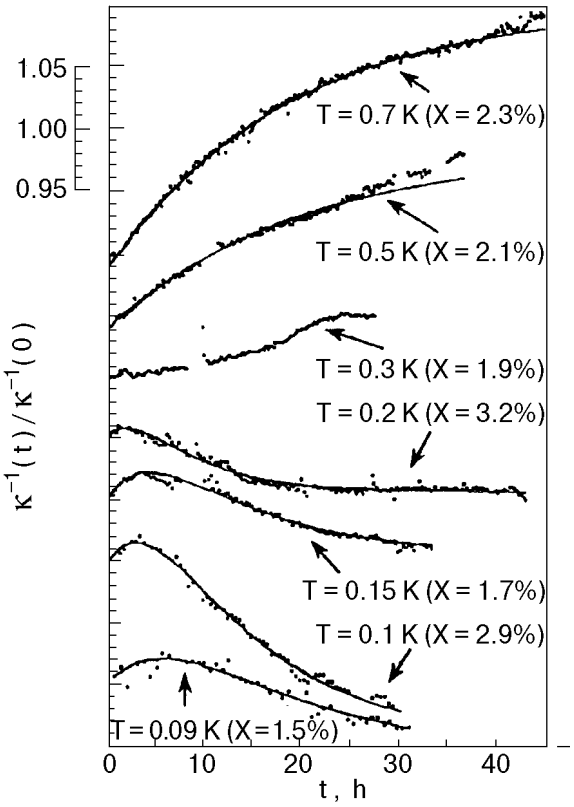

Fig. 4. Normalized thermal resistivity $\kappa^{-1}(t)/\kappa^{-1}(0)$ versus time at several temperatures for samples grown at constant density. To avoid overcrowding, the origin of the vertical scale for the various isotherms has been shifted from 1.00. The solid lines are fits of exponential transients to the data, as described in the text (after Ref. 21).

ity of a pure $(J = 0)H_2$ crystal and represents the phonon scattering by the lattice as determined by grain boundaries, lattice imperfections etc. The second term, $\kappa^{-1}_{(J=1)H_2}(X, T)$ is the contribution from the inelastic phonon scattering by the excitation of the rotational energy states in the $(J = 1)H_2$ molecules. During the clustering process, we expect $\kappa^{-1}_{(J=1)H_2}(X, T)$ to change as a function of time.

The experiments were carried out in a special thermal conductivity cell made of a proton-free commercial plastic, «Kel-F», that enabled the NMR spectrum to be scanned continuously while conductivity measurements were performed automatically as a function of time. The cell was cooled rapidly from a standard temperature, usually 2.2 K, where clustering is small, to a final temperature T_{fin} which was then stabilized for periods up to 45 h. During this time data on the conductivity and on the central NMR line amplitude, the latter being the signal of the «isolated» $(J = 1)H_2$, were recorded. A sample of the results, suitably normalized to the initial observed resistivity $\kappa^{-1}(0)$ is shown in Fig. 4 for the earlier experiments [21] with the samples grown at constant density. Figure 5 shows a repre-

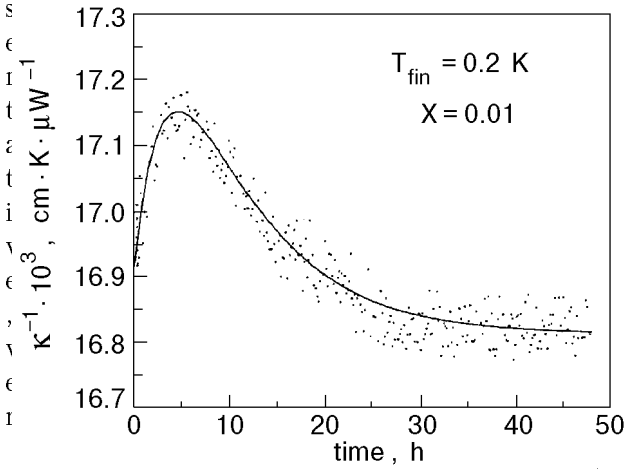

Fig. 5. A representative time evolution of the resistivity κ^{-1} at $T = 0.2$ K and $X(J = 1) = 0.01$ obtained with a sample grown at constant pressure. This should be compared with the curve for the same temperature in Fig. 4. The solid line is again a fit of exponential transients to the data (from Ref. 22).

ly expanded time profile for $\kappa^{-1}(t)$ for $X = 0.01$ and $T_{fin} = 0.20$ K, obtained with the sample grown at constant pressure [22]. The curve is similar to that in Fig. 4 for the same T_{fin} . In both figures,the solid lines are fits to a sum of two exponential terms,

$$\kappa^{-1}(t) = A + B \exp(-t/\tau_1) + C \exp(-t/\tau_2) . \quad (3)$$

The thermal transport and NMR data show remarkable features, the two principal ones being as follows:

a) Thermal resistivity change. Above $T \approx 0.3$ K, the resistivity increases as clustering proceeds. The equilibration can then be represented approximately by a single exponential term with a time constant τ_1 . The change $\Delta\kappa^{-1} = [\kappa^{-1}(t = \infty) - \kappa^{-1}(0)]$ is positive, $\Delta\kappa^{-1}$ decreases and changes sign near 0.3 K. The time profile of $\kappa^{-1}(t)$ becomes more complex with decreasing temperature, first rising and then decreasing to its equilibrium value. As a result, $\Delta\kappa^{-1}$ becomes negative. This is shown in Fig. 6 where the results at Kharkov obtained by Gorodilov et al. [24], the predictions by Kokshenev at high temperatures [25] and the published [21] and unpublished [22] data in this laboratory are shown. (The single data point obtained in Ref. 26 has been omitted.) Given the various uncertainties, there is good consistency between the various measurements. The unexpected behavior change in sign of $\Delta\kappa^{-1}$ near 0.3 K is therefore confirmed.

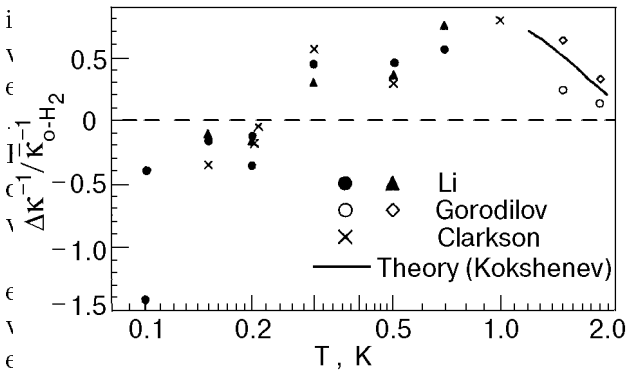

Fig. 6. The normalized change $\Delta\kappa^{-1}/\bar{\kappa}^{-1}_{(J=1)H_2}$ versus T for two series of experiments where $\bar{\kappa}^{-1}_{(J=1)H_2}$ is the average resistivity of the $(J = 1)H_2$. Solid circles: $1.5\% < X < 3.4\%$, solid triangles: $0.9\% < X < 1.1\%$ from Ref. 21. Open circles and diamonds: for $X = 1$ and 2% from Ref. 24. Crosses: $1.0\% < X < 2.5\%$ from Ref. 22. The solid line is the prediction by Kokshenev [25] for $X = 1\%$.

b) Relaxation times. The transients shown by the exponential decay of the «isolated» $(J = 1)H_2$ (from NMR) and by the change of conductivity, and measured simultaneously on the same sample, show different relaxation times. This is illustrated in Fig. 7 for a representative temperature above $T = 0.3$ K. While both observations reflect clustering, they represent different aspects: the NMR shows the signal of «singles» decaying with time, while measurements of thermodynamic averages such as heat capacities and thermal conductivity reflect the complicated dynamics of $(J = 1)H_2$ cluster formation (pairs and larger groups). In Fig. 8 the relaxation times from NMR measurements are presented together with those from C_p and from κ. For simplicity, I do not show the data from conduc-

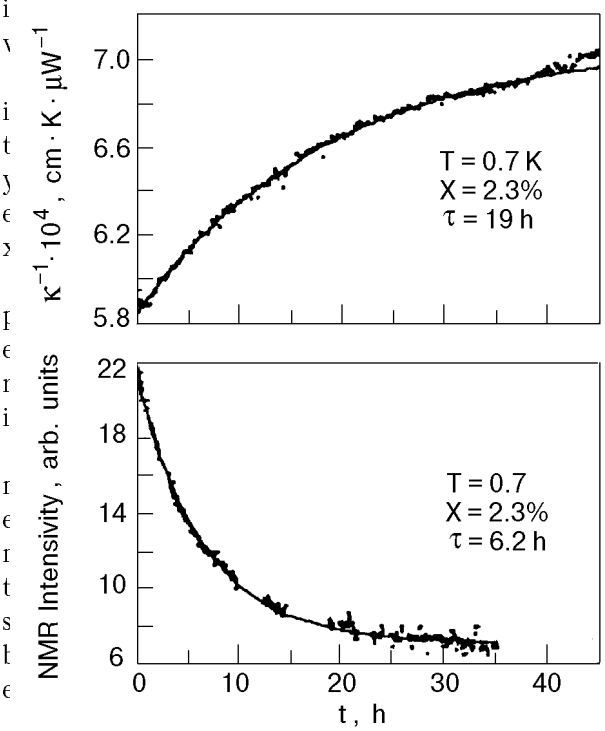

Fig. 7. Simultaneously recorded thermal resistivity and NMR signal intensity versus time at 0.7 K (from Ref. 21).

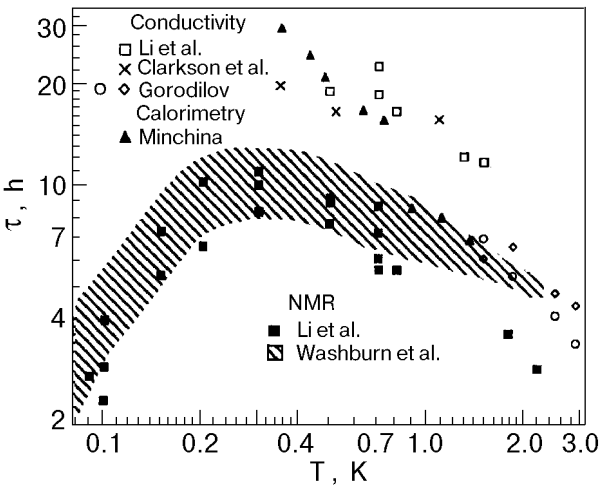

Fig. 8. Observed configurational relaxation times τ from various experiments in pure solid H_2. Solid squares NMR, isolated $(J = 1)H_2$; open squares: conductivity, obtained during simultaneous experiments [21]. Open circles and diamonds: conductivity from Ref. 24. Crosses: conductivity with sample grown under constant pressure (from Ref. 22). Solid triangles: calorimetry from Ref. 14. The shaded area includes the NMR results on isolated $(J = 1)H_2$ impurities (Ref. 13).

becomes rather complex, with the formation of «pair» clusters that subsequently hop and congregate to form larger clusters (see Fig. 7,*b* in Ref. 21). Based on the evidence from NMR data [13] that describe the decay rate of $(J = 1)H_2$ pairs into larger $(J = 1)H_2$ clusters, and which accelerates with decreasing temperature, it is reasonable to expect that the clustering relaxation times observed in calorimetric and thermal conductivity experiments will pass over a maximum and decrease with decreasing temperature below 0.3 K.

As can be seen from Fig. 8, the characteristic clustering times τ obtained from NMR in both experiments performed at zero pressure [13] and at a pressure of approximately 90 bar [21] agree within the considerable experimental scatter. The *resonant* $(J = 1) \leftrightarrow (J = 0)$ *conversion* mechanism [11] leads to the prediction of a roughly 10% increase in the hopping frequency for a density increase of 5%, which corresponds to a pressure change from 0 to 100 bars. This pressure effect might be too small to detect, given the scatter in the measurements of τ. By contrast, *mass quantum diffusion* of $(J = 1)$ impurities, as produced by the motion of three-body cyclic permutation in the $(J = 0)$ lattice [27] is predicted to decrease by a factor of 60 for this 5% density increase. Therefore the observations mentioned above favor resonant conversion over tunneling as the dominant mechanism of quantum diffusion, at least below 4 K.

The thermal transport measurements can be summarized as follows: at temperatures above ≈ 0.5 K, the time dependence and the sign of the resistivity κ^{-1} after a temperature quench to T_{fin} indicate that clustering of isolated «single» $(J = 1)H_2$ particles takes place, but as T_{fin} is decreased, there appears to be competition between several clustering variations, and the time dependence of κ^{-1} becomes more complex. It is probable that clustering into larger configurations causes the trend of $\kappa^{-1}(t)$ to change direction. The initial increase of $\kappa^{-1}(t)$ — which reflects the simple clustering of single particles — is compensated within a few hours after the temperature quench and is exceeded in magnitude by the effect from the clustering of larger groups. The quantitative understanding of this phenomenon remains to be clarified.

3. Theory on the pairing of $(J=1)H_2$ *impurities.* Significant progress has been made in recent years in the understanding and the simulation of the pairing procedure of $(J = 1)H_2$ particles in a solid $(J = 0)H_2$ matrix [28–30]. As already calculated by Oyarzun and van Kranendonk [11] and discussed by van Kranendonk [15], the order of magnitude of resonant $(J = 1) \leftrightarrow (J = 0)$ conversion «hopping» frequency ν_0 for an «isolated» $(J = 1)H_2$ surrounded only by $(J = 0)H_2$, is of the order of $1 \cdot 10^3$ s^{-1}. Electrostatic quadrupole-quadrupole interactions with $(J = 1)H_2$ neighbors produces randomly fluctuating orientations, corresponding to an energy band width that increases rapidly as $X(J = 1)$ increases. This reduces the probability of an energy-conserving jump. For $X = 10^{-2}$, the reduction factor is calculated to be 10^{-7}, hence the hopping frequency is only $\nu(X = 0.01) = 5 \cdot 10^{-5}$ s^{-1}. Meyerovich and collaborators note that this small frequency ν_0 is very sensitive to inhomogeneities of the potential relief $U(\tau) \approx U_0(a/\tau)^5$, where $U_0/k_B \approx 0.8$ K, and depends on the orientation. They explore the existence of a strong directional bias, which will influence the time where one $(J = 1)H_2$ impurity approaches another one to form a pair. Stimulated partly by the observation of the maximum in the characteristic time of pair formation near 0.3 K [13,31], Meyerovich advanced the idea that a directional bias might lead to such a maximum even if the individual hopping rates should show a monotonic behavior with T, i.e., an increase as T decreases. The two energy-conserving mechanisms for enabling hopping in the presence of an energy mismatch $\varepsilon_{i,j} = U(r_i) - U(r_j)$ from site i to site j are a) spontaneous emission of phonons with an energy $\hbar\omega/2\pi = \varepsilon_{i,j} > 0$, and b) inelastic scattering of thermal phonons. The former process is only possi-

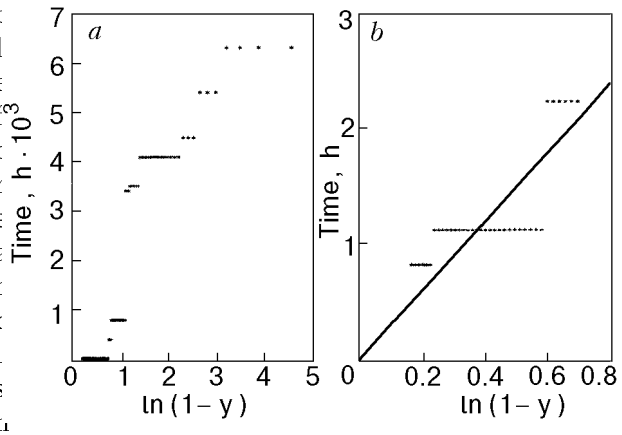

Fig. 9. The fraction y of pairs versus time (in hours) for a cell size with 100 lattice sites, corresponding to $X(J=1) = 1 \cdot 10^{-2}$, pictures the pairing of 88 impurities, each marked by a symbol (*). a) overall picture; b) the initial stage of pairing of 38 impurities (after Fig. 2 of Ref. 30. It is from the initial stage that the pairing time is derived by the slope of the straight line.

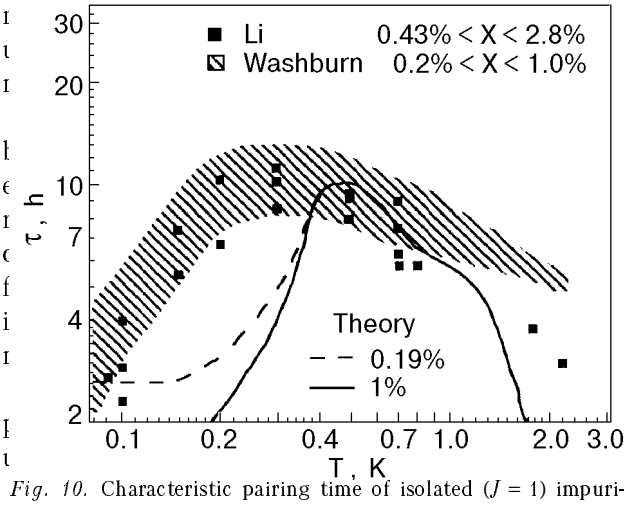

Fig. 10. Characteristic pairing time of isolated ($J = 1$) impurities. The shaded area represents the NMR data monitoring the signal decay of the «isolated» ($J = 1$) impurities [13,21]. The solid and dashed lines represent an average of the predictions for $X = 10^{-2}$ and $1.9 \cdot 10^{-3}$ (after Ref. 29).

isotropic, while the latter operates for any sign of $\varepsilon_{i,j}$. When $\varepsilon << h\omega_0/2\pi$, the hopping time is much larger than that calculated for phonon-assisted hopping and is given by ω^{-1}. The authors calculate the average pairing time with the help of a computational model for $X = 10^{-2}$ and 10^{-3}. One ($J = 1$) impurity is moving while all the others, randomly distributed, stay fixed. The single particle diffuses in the cell and can pair with any one of the immobile impurities. The motion of the particle is tracked and the times of hopping are adjusted as the energy mismatch $\varepsilon_{i,j}$ and particle distribution change. In the calculation, hcp lattices with 100 to more than 10^3 lattice sites per cell were generated when the concentration decreased from about $X = 10^{-2}$ to 10^{-3}.

The calculation gave the number of paired impurities as a function of time, assuming a random initial distribution of impurities over all sites, except at the origin, from where the diffusing particle starts, and its nearest neighbors. However, instead of a smooth curve indicating the pairing process to be exponential with time and characterised by a time τ, the plot gave a staircase (Fig. 9) which the authors interpreted to indicate that the pairing process is characterised by a set of times rather than by a single τ. They speculated that the staircase should become smoother when account is taken of an averaging effect by the motion of other particles. For their choice of a characteristic time τ, the authors used the time profile $t(n)$ describing the initial stage of pairing (the first step of the staircase). Here $n = N/N_T$, where N is the number of impurities that have been paired and N_T is the total

es considered in the calculation. In a plot versus temperature, they show that this time τ passes over a maximum near $T = 0.4$ K. By contrast, the characteristic time of the final stage of pairing is much longer and steadily increases with decreasing T. The authors then discuss in detail the numerical value of the two independent parameters in their calculations that produce a reasonable fit with experiment. They find, for instance, that the temperature position of the maximum in τ is rather insensitive to the value of (ξ_1/ξ), where ξ_1 and ξ are constants appearing in the expression for the time of the phonon-assisted impuritiy hopping. The lower bound of the estimate for ν_0 coincided with the value [15] 10^3 s^{-1} while the upper bound was about two orders of magnitude higher.

In Fig. 10 we present experimental data and theoretical curves from Ref. 30. Two unknown computation parameters (bare tunneling frequency ν_0 and a coefficient in its temperature renormalization) were chosen so as to fit the position and height of the maximum $\tau(T)$ to experimental data. The main difference between experimental data and computational results is in the position of the maximum. In principle, the theoretical curve should be shifted to the left by 0.2 K, from 0.5 to 0.3 K, and stretched vertically to make experimental and theoretical maxima coincide. This procedure should improve agreement between experimental and theoretical data. However, the position of the maximum and the shape of the curve were not very sensitive to the fitting parameters, and such a shift would require changing the unknown renormalization coefficient by an order of magnitude away from its expected

range [17]. On the other hand, this insensitivity is a good sign demonstrating that the existence of the maximum is a stable general phenomenon. Better agreement with experimental data requires improvement of an over-simplified computational model [30].

The numerical calculation leads to the following conclusion, as stated by the authors [29]: the low temperature peak in the characteristic pairing time is caused by a directional bias in the diffusion, which is conditioned by the interaction mechanism of the pairing particles with the surroundings. One of the diffusion mechanisms — the hopping with inelastic phonon scattering — is biased against mutual approach of the particles and opposes pairing. When this mechanism dominates at temperatures above the maximum in τ, a decrease in the temperature results in a slow-down in motion, including the pairing. As T further decreases, a temperature-independent motion with emission of phonons becomes increasingly important, and this neutralizes the first mechanism and increases the pairing rates.

So far, theory has considered the clustering dynamics from an isolated ($J = 1$) impurity to the final paired state. The statistical mechanics aspects (equilibrium concentration of pairs at a given temperature, as based on the Free Energy minimum) were ignored within the considered model with single-particle motion. The theory assumes all single impurities will cluster, which should be nearly realized only below ≈ 0.5 K.

Furthermore I note that the calculation of the characteristic clustering time τ has been made from the initial pairing stage, as computation of τ from the later stages gave a substantiallly larger value. The experimentally observed transient of the «single» ($J = 1$) signal $[n(t) - n(t = \infty)]$ followed an exponential decay all the way, and not just in the initial stages, as shown by all the NMR experiments [4,13,21]. It is hoped that in the near future these problems in the theory can be addressed.

C. *Tunneling of* HD *and of* $(J = 1)H_2$ *in solid* H_2

There has been considerable activity in the study of low-temperature tunneling motions, both of molecules (HD) and of atoms in a matrix of solid H_2. (This process of motion is, of course, different from quantum diffusion resulting from ortho-para resonant conversion in H_2 and in D_2.) Furthermore experiments have been reported on H_2^- anion tunneling (see Section 2D). First the detailed NMR studies by the group of Sullivan, showing evidence of HD tunneling, will be described. This will be

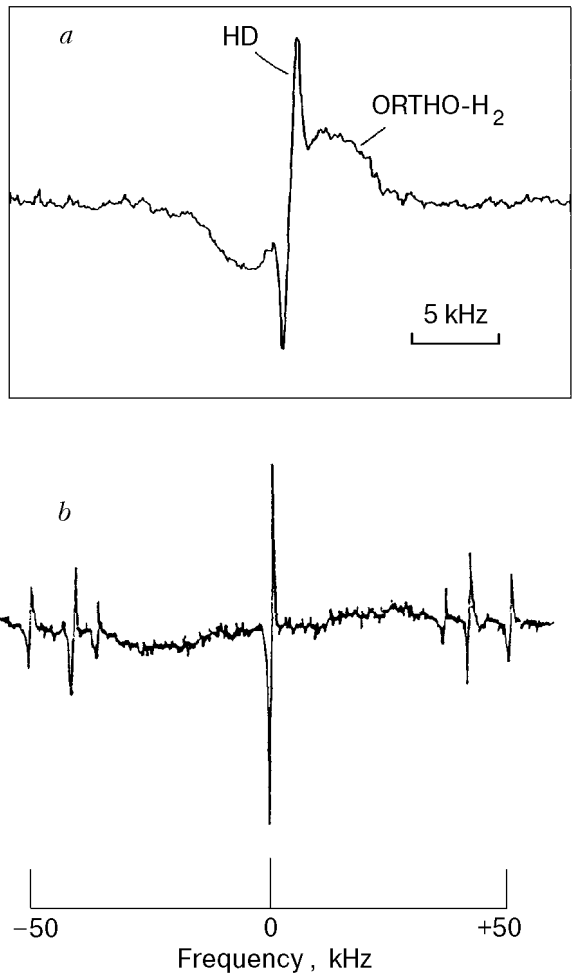

Fig. 11. a) The NMR derivative line shapes of the proton spectrum of HD (1.1%) and $(J = 1)H_2$ ($X = 0.018$) in solid $(J = 0)H_2$ at temperatures below 4 K, where they can be separated (from Ref. 34). b) Well resolved spectra of HD (0.04%), center line, and $(J = 1)H_2$ pair spectra for $x = 0.8\%$ at $T \simeq 30$ mK (from Ref. 37).

nt that indicates tunneling motion of $(J = 1)H_2$.

1. HD *tunneling from NMR experiments.* Pulse measurements [32–35] were carried out at 268 MHz and both the longitudinal and the transverse relaxation times, T_1 and T_2, of the proton nuclei were measured. The samples consisted of HD and of $(J = 1)H_2$ impurities in a matrix of solid $(J = 0)H_2$. The most extensively studied sample contained 1.1% of HD and 1.6% of $(J = 1)H_2$. Although the proton line shapes of HD and H_2 can only be resolved below ≈ 4 K (see Fig. 11), they have very different relaxation times. Therefore the respective signal contributions can be separated and this is most striking for T_1. It is known that the spin-lattice relaxation time in pure H_2 for such low $(J = 1)H_2$ concentrations is of the order of ms and has only a weak temperature dependence. (See, for instance, Ref. 36 and references therein.) The char-

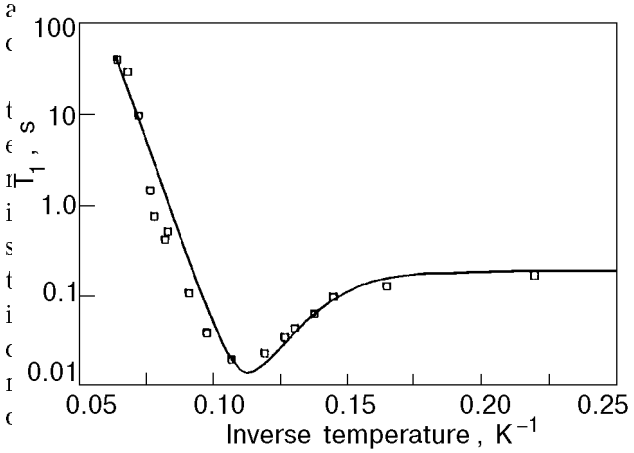

Fig. 12. The observed and calculated temperature dependence of the spin-lattice relaxation time T_1 of the HD impurities (1.1%) in H_2 with $X(J = 1) = 1.8\%$. Symbols: data of Rall et al. [34]. Solid curve: theory [35].

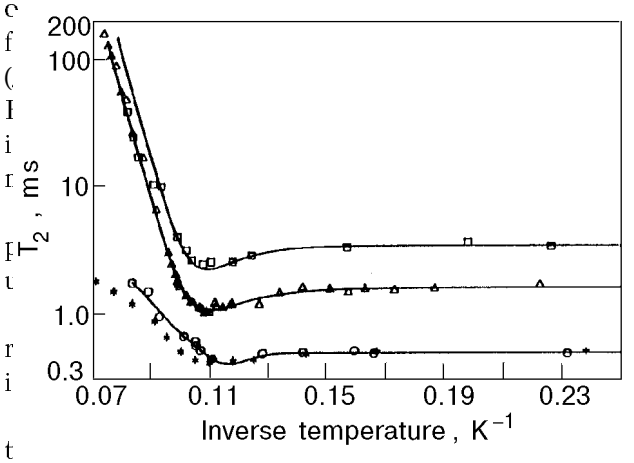

Fig. 13. Observed temperature dependence of the transverse nuclear relaxation time T_2 from the proton signal of HD and $(J = 1)H_2$ impurities in solid $(J = 0)H_2$ for three different samples. Squares: 1.1% HD, 1.8% $(J = 1)H_2$; triangles: 1.1% HD, 2.1% $(J = 1)H_2$; circles: 0.05% HD, 2.5% $(J = 1)H_2$ (after Ref. 34). (The data represented by the asterisks are from Ref. 36.)

lar orientation fluctuation frequency spectrum ω_Q from the intermolecular electric quadrupole-quadrupole interactions modulate the dipolar interaction between the two protons. For $(J = 1)H_2$ concentrations of a few percent, $\omega_Q/2\pi$ is comparable to the Larmor frequency of the order of 10 to 10^2 MHz, and this favors rapid energy transfer from the spin «bath» to the rotational energy bath, and from there to the lattice. The protons of HD do not have this mechanism of energy transfer, and their intrinsic relaxation rate to the lattice is very slow. However, as shown in Ref. 35, the cross-relaxation from the HD spin system to that of $(J = 1)H_2$ permits a faster relaxation. Furthermore, this mode of energy transfer is sensitive to the motion of the HD molecule. In the high temperature regime (for $T > 11$ K), the mechanism of cross-relaxation is attributed to the motion of vacancies, while in the low temperature regime ($T < 8$ K), quantum tunneling of HD impurities is the responsible mechanism.

The longitudinal relaxation time measurements showed a pronounced minimum (Fig. 12) which was analyzed in Ref. 35. Starting from the low temperature end, where the cross-relaxation time is nearly constant and is determined by the quantum tunneling frequency J of the HD particles, impurity scattering with an activation energy E_F becomes important and leads to a decrease of T_1 . The progressive excitation of vacancy motion with an activation energy E_B then pulls up T_1 as the temperature increases. The theory is thus able to account for the observed minimum. The quantum tunneling frequency so derived is $J = 1.3 \cdot 10^3$ Hz, which is of the same order as the hopping frequency

resonant conversion [15]. The energies obtained by fit to the data are $E_F/k_B = 91$ K and $E_B/k_B = 100$ K. It is the sum $(E_F + E_B)/k_B$ that determines the limiting high temperature slope seen in Fig. 12, and which agrees with previous determination of the activation energies in $(J = 1)H_2$. It should be noted that in pure solid H_2 with such low values of $X(J = 1)$ as used here, this temperature dependence of T_1 is not observed, but the addition of HD impurities leads to a temperature profile of both T_1 and T_2 — a pronounced minimum and a sharp rise with T — and permits the separate determination of these activation energies.

The transverse relaxation times show a similar behavior to the longitudinal ones, but with a less pronounced minimum. Figure 13 shows a representative curve for T_2 with 1.1% HD and 2.1% $(J = 1)H_2$ between 15 and 4 K [34]. There is a weak linear temperature dependence below 4 K where T_2 rises to ≈ 3 ms near 0.1 K (Fig. 4 in [34]). Again the results could be interpreted by quantum diffusion of the HD impurities at temperatures below ≈ 6 K. This value of T_2 is higher than calculated for HD in a rigid H_2 lattice, and this leads to the conclusion that diffusion narrows the linewidth (or raises T_2). As the temperature increases, first vacancy-impurity scattering with an activation energy $E_B/k_B = 91$ K, and then vacancy motion with an activation energy $(E_B + E_F)/k_B = 196$ K explain the data very well. Neglecting the small temperature dependence that is attributed to formation of $(J = 1)H_2$ clusters at temperatures below 4 K, the diffusion coefficient can be represented by

antum + D_0^{classic} e^{-E_B/k_BT} e^{-E_B/k_BT}

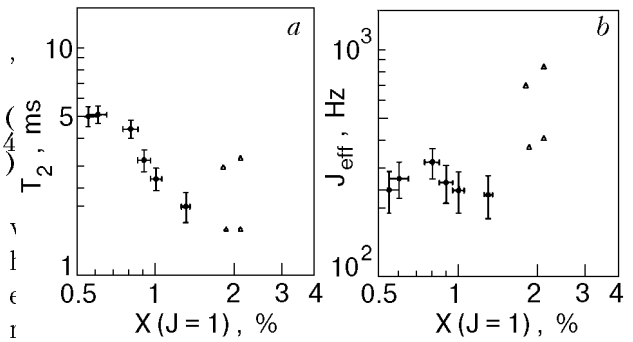

Fig. 14. a) The T_2 data in the temperature range of 50–100 mK as a function of $X(J = 1)$. Solid circles with error bars from Ref. 38, triangles: from Figs. 3 and 4 in Refs. 34, 39. b) The derived tunneling frequency J_{eff} versus $[X(J = 1)]$, as obtained from the T_2 data via equations (9)–(11) (in Ref. 34).

$D_0^{\text{quantum}} = 1.6 \cdot 10^{-8}$ cm^2/s

$D_0^{\text{classic}} =$

$= 5.9 \cdot 10^{-3}$ cm^2/s

. From the value of D_0^{quantum}, the authors calculate a tunneling frequency of $J_{\text{eff}} =$ $= 1.5$ kHz. (See, however, the revised analysis below.)

Rall et al. [34] pointed out that it would be valuable if both results obtained at Duke University and at the University of Florida could be compared at the same temperature. In fact such a comparison can be made readily for the temperature range below 0.1 K, where the temperature dependence of T_2 is only weak, and is based on the experiments carried out at Duke [37,38] as presented in Ref. 38. The details of this comparison and their analysis to obtain the tunneling frequency J are deferred to the Appendix. Briefly, the result is that the T_2 data obtained in both laboratories under comparable conditions of $X(J = 1)$ of temperature and of r.f. pulse length are of the same order. The uncertainty lies in the analysis of T_2 to obtain the tunneling frequency. This frequency, when derived with the use of the relations reviewed in the Appendix, is lower than the $J_{\text{eff}} = 1.34$ kHz claimed by Rall et al. [34]. While tunneling of HD in the matrix of $(J = 0)H_2$ no doubt exists, its frequency, as obtained from the Duke data, is of the order of $3 \cdot 10^2$ Hz, and independent of $X(J = 1)$ and of T within the experimental uncertainty. The reanalyzed UF data [39] give $J_{\text{eff}} \approx 800$ Hz. The results are shown in Fig. 14,*b* where the DU and the UF data are compared.

2. Enhanced ortho–para conversion in solid H_2 *with* O_2 *impurities*

Tunneling appears also to be important in the $(J = 1) \rightarrow (J = 0)$ conversion in solid H_2 catalyzed by O_2 impurities, as shown by Shevtsov et al. [40]. Here the conversion rate for small concentrations of O_2 was studied between 4.2 and 7 K. The authors report a very different conversion rate (magnitude, as well as temperature dependence) from that for pure solid H_2 . Diffusion of $(J = 1)H_2$ is invoked, and a fit of the proposed model to the data gives a diffusion coefficient $D(T) = D_0 \exp(-96/T)$. The activation energy is comparable to that obtained by the group of Sullivan for the HD tunneling in this temperature region, where the potential energy of (91 ± 6) K was attributed to impurity-vacancy scattering [35]. The prefactor $D_0 = 3 \cdot 10^{-11}$ cm^2/s corresponds to a tunneling frequency ~ 10^3 times smaller than that for HD and smaller than ν_0 for the resonant $(J = 1) \leftrightarrow (J = 0)$ conversion of an isolated pair in $(J = 0)H_2$ [15], where ν_0 is of the order 10^3 s^{-1}.

D. Tunneling of D *or* H *atoms and* H_2^- *anions in solid* H_2

A very interesting development over the last fifteen years is the systematic study of low temperature chemical reactions. Here electron spin resonance techniques are used to observe the H or D signal intensity in a matrix of solid H_2 , HD or H_2–D_2 mixtures. The atoms are produced by the irradiation of the solid sample by γ rays from a Co^{60} source or with x-rays, and their ESR signal shows an exponential decay with time that is interpreted as recombination through tunneling. This research elucidates chemical kinetics near 4 K and below, where all the thermally activated reactions are suppressed, and only those driven by quantum tunneling take place.

A major portion of this research has been carried out at Nagoya University by the group of Miyazaki, and a review of papers before 1990 has been presented by him in Ref. 41. Among the many reactions studied experimentally and also theoretically, a very interesting one has been the irradiation of a solid D_2–HD mixture by γ rays at 4.2 K [42]. Simultaneous ESR measurements of H and D atoms, made after the irradiation, showed clearly the D signal to decrease while that of H increased with time. The results indicated convincingly the occurence of the reaction

$$HD + D \rightarrow H + D_2 \,. \qquad (5)$$

The signal transient curve obtained for $T = 4.2$ K was found to be the same at 1.9 K, indicating that the reaction rate was temperature independent. Because the potential barrier for this reaction is $\Delta E/k_B \approx 5 \cdot 10^3$ K, the reaction cannot occur by thermal activation, but must take place by quantum

tunneling. Several types of calculations of the rate constants in this tunneling regime have been carried out and were listed in Miyazaki's review. In a review of more recent papers [43], the temperature dependence of the above reaction has been investigated in detailed fashion and shows a dramatic temperature dependence of the reaction constant k defined by the relation

$$\frac{d[\mathrm{D}]}{dt} = -k[\mathrm{D}][\mathrm{HD}] \ , \qquad (6)$$

where the components in brackets signify the fraction of the reactants.

This behavior of k is shown in Fig. 15 where k sharply decreases with falling temperature as thermal activation becomes frozen out. Below 4 K, k remains constant. From the temperature dependence between 6.5 and 5 K, the authors [44] derive an activation energy $\Delta E/k_B = 95$ K, which is similar to values between 85 and 105 K obtained for vacancy diffusion in solid HD from NMR transverse relaxation time measurements [34]. This result is discussed in terms of the distortion of the solid hydrogen lattice structure by the H and the D atoms, which is caused by the large zero-point vibration of these atoms. The authors argue that in the tunneling process, the deformation accompanies the atoms. When a vacancy moves to another site by thermal activation, the atom tunneling is accelerated by the vacancy motion. This is vacancy-assisted tunneling reaction, which becomes temperature-independent below about 4 K. Investigation of the ESR fine-structure and the linewidth for H atoms in solid HD furthermore gave information on the distance between the tunneling atom and the nearest neighbor molecules. It was found that the average distance H–HD was ≈ 3 Å.

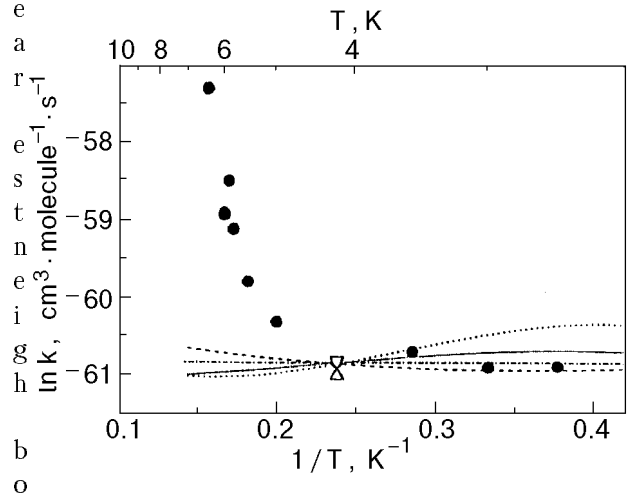

Fig. 15. The rate constant k for the tunneling reaction $HD + D \rightarrow H + D_2$, solid circles, open triangles: experimental data; curves: calculations based upon different potential surfaces (after Ref. 43).

Another interesting investigation is that of the decay rate of H_2^- anions [45]. In the reaction accompanying the decay, the anions change into electron bubbles, as represented by the equation

$$H_2^- + HD \rightarrow H_2 + HD + e^-_{\text{bubble}} \ . \qquad (7)$$

The ESR spectrum of electron bubbles has been observed to become more intense while that of the H_2^- decreases. The decay rate constant has a rather striking temperature dependence,as shown in Fig. 16. Here solid $(J = 0)H_2$ has been irradiated with x-rays. The measured decay rate constant can be represented by a sum of two terms. The first is a thermally-activated process above 5 K with an activation energy of $\Delta E/k_B = 93$ K, the same as in the reaction given by Eq. (4). The second term is a phonon scattering process in quantum diffusion. The tendence of the decay rate constant towards temperature independence below 3.2 K might indicate quantum diffusion in the absence of phonon scattering. The possibility has been raised [45] that the origin of anion motion might be through reaction with a tunneling impurity HD molecule. However another mechanism of anion hopping is given by the conversion

$$(J = 0)H_2^- + (J = 0)H_2 \rightarrow (J = 0)H_2 + (J = 0)H_2^- \ . \qquad (8)$$

Because of the light mass of the excess electron, and the symmetry between the initial and final compound, this conversion might occur by quantum tunneling even at relatively high temperatures.

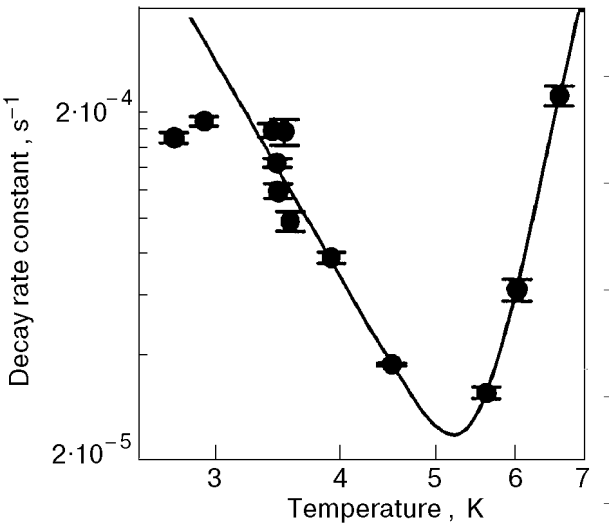

Fig. 16. The decay rate constant of H_2^- anions in x-ray irradiated solid $(J = 1)H_2$ over the temperature range 2.7–6.6 K. The solid curve shows a two term fit to the data, as explained in the text (after Ref. 45).

tron. However information on the anion H_2^- in solid H_2 is insufficient so far to permit more discussion.

3. Conclusion

Much progress has been made in the past ten years in the understanding of quantum diffusion and tunneling phenomena in the solid hydrogens. It is hoped that this review will stimulate further investigations in several areas. Since the tunneling study of HD, H and D atoms in solid hydrogen is a very active subject of research at present, I restrict myself to the topic of $(J = 1)H_2$ quantum diffusion through the resonant conversion process.

i) More and better NMR experiments are certainly needed with dilute mixtures below 0.1 K to explore whether the clustering time τ tends to a constant value, as suggested by theory.

ii) Although the theory of single-particle clustering is already quite complex, it is hoped that still further improvements can be made to bring theory into better agreement with experiments and to clarify the problem of the transient decay, which is observed to be exponential during the whole process and not only in the initial stages of clustering.

iii) The complicated time dependence of the thermal resistivity after the quench to a final temperature T_{fin} needs to be quantitatively explained as a function of T. It would be interesting to find out whether calorimetric experiments also show a complex time dependence at temperatures below 0.5 K after a temperature quench.

iv) There is also the intriguing question of what happens to clustering at larger $(J = 1)$ concentrations than a few %. Pressure experiments [12] at constant volume, $P_V(t)$, suggest that as $X(J = 1)$ increases, the clustering time decreases. Could quantum diffusion play a role in the martensitic transformation (from $Pa3$ cubic to hexagonal close packed) that accompanies the orientational order–disorder transition? The transformation, which is observed for $X(J = 1) > 0.55$, has been known for about thirty years and is very different for solid H_2 and D_2. The dynamics of the thermal cycling and phase stability for this transition have been recently reviewed [46]. While the effect of quantum diffusion on the irreversible $(J = 1) \rightarrow (J = 0)$ conversion rate can be observed in various types of experiments at low concentrations when clustering has occured, it also appears that diffusion at intermediate concentrations is still efficient in bringing about a random distribution of the $(J = 1)H_2$ in the matrix as the conversion proceeds. It is difficult to observe directly this diffusion from $P_V(t)$ measurements, because the time dependence of P_V from the $(J = 1) \rightarrow (J = 0)$ conversion masks any molecular rearrangement effect due to diffusion.

This short review has been restricted to the solid hydrogens in three dimensions. The very interesting subject of molecular motions in thin films of H_2, HD and D_2 has received much attention, especially over the past ten yeats, and a review on this topic is certainly due. For the reader's convenience I list some of the recent works [48–51] where references to previous research in this field are given.

4. Dedication and Acknowledgments

This review is dedicated to the memory of Neville Robinson (1925–1996), whose gift of several «Robinson» spectrometers was crucial both in the NMR research that led to the first observation of clustering in solid H_2 and to its further study over the next 20 years, and also in my Undergraduate Advanced Physics Laboratory at Duke University.

My thanks go to my former associates L. I. Amstutz, J. R. Thompson, D. Ramm, S. Washburn, R. Schweizer, I. Yu, X. Li, and D. Clarkson who contributed significantly to the study of quantum diffusion at Duke University.

I have profited greatly from stimulating interaction with A. M. Meyerovich, N. S. Sullivan, and S. Washburn who gave detailed advice on a draft of this paper. In particular I am grateful to the first two for clarifications and discussions of several aspects of their papers.

Also my sincere thanks go to D. Murphy for recasting several of the figures into a presentable form.

V. Appendix: The HD hopping frequency as derived from T_2 measurements

First I review the data for the transverse relaxation time T_2 obtained at the University of Florida (UF) and at Duke University (DU) under comparable experimental conditions. This is followed by a data analysis to obtain the HD tunneling frequency.

It might be noted that for the HD spins, the statistical rigid-lattice NMR full width at half maximum (FWHM) is given by $\Delta_{FWHM} = 63.4\, X(J = 1)$ (kHz) in Ref. 34. The numerical coefficient is larger by a factor of about 3 than that presented in Ref. 37, Eq. (7a), and which was based on a model by Delrieu and Sullivan [27]. (This width was denoted by δ/π in Refs. 27 and 37.) The new value of Δ_{FWHM}, which is larger than the experimental one deduced from T_2 data, indicates «motional narrowing» of the (Lorentzian)

line, and signifies that HD tunneling is taking place.

The data at UF were obtained with r.f. pulse amplitudes giving a field of 15 G in the rotating frame [34]. For a $\pi/2$ pulse, this corresponds to a pulse length of ≈ 4 μs. In the DU experiments [37,38], pulse lengths for a $\pi/2$ pulse were between 11 and 100 μs and the T_2 results were extrapolated to zero pulse length. The UF sample concentrations were $C(\mathrm{HD}) = 1.1\%$, $X(J = 1) = 2.1\%$ and $C(\mathrm{HD}) = 1.1\%$, $X(J =)1.8\%$. Those of the DU sample IV were $C(\mathrm{HD}) = 0.04\%$ and $0.55\% < X < 1.3\%$, where $X(J = 1)$ decreased through conversion over the period of the experiment. The data taken near $T = 50$ mK are shown in Fig. 14,*a*. Because of the significant dependence of T_2 on pulse length [37,38], the DU T_2 data near $X = 1.3\%$, converted to 4 μs pulse length, would have been respectively ≈ 0.7 ms larger than for zero pulse length, namely ≈ 3.1 ms, which is comparable with the data obtained at UF, namely 3.4 ms for $X(J = 1) = 2.1\%$ and 4.6 ms for $X(J = 1) = 1.8\%$.

The next step, the calculation of the HD jump frequency, has uncertainties which were discussed previously [37]. The difficulty lies in the correct choice of the rigid lattice second moment of the HD line for low values of $X(J = 1)$ and in the presence of clustering. It is therefore interesting that for short $\pi/2$ pulses of 11 μs or less, T_2 does not seem to change significantly as clustering proceeds in time (Fig. 4,*a* in Ref. 38 and Fig. 4 in Ref. 34).

For the sake of comparing the data of UF and DU in a consistent way, I use Eqs. (18), (28), and (30) in the paper by Rall et al. [34].(Note: the «X» in the denominator of Eq. (18) should be suppressed [39].) The tunneling frequency J_{eff} is then given by

$$J_{\mathrm{eff}} = \frac{4T_2 M_2^{\mathrm{HD}}}{6\pi} \qquad (9)$$

where the second moment M_2^{HD} of the HD rigid lattice NMR line is given by

$$M_2^{\mathrm{HD}} = \left[\frac{3}{8}\frac{C(\mathrm{HD})}{X(J=1)} + \frac{4}{9}\right] M_2^{\mathrm{H}_2}(X) \; . \qquad (10)$$

Here $M_2^{\mathrm{H}_2}$ is the second moment of the H_2 line. For this quantity the high temperature limit value under the assumption of random $(J = 1)H_2$ distribution [[47] was taken,

$$M_2^{\mathrm{H}_2}(X) = 90X\ (\mathrm{kHz})^2 \; . \qquad (11)$$

Inserting the respective values of $X(J = 1)$ and $C(\mathrm{HD})$ into the equations, the values of J_{eff} are obtained as shown in Fig. 14,*b*). There appears to be no significant variation of J_{eff} with $X(J = 1)$ in the DU experiment, but a discrepancy exists with the results from the UF group which is diminished if one takes into account the pulse length-dependence of T_2, as discussed above. The UF values for J_{eff}, quoted here after clarifications by Sullivan [39], are lower than 1.34 kHz, reported in the paper of Kisvarsanyi and Sullivan [35].

1. H. Meyer, *Can. J. Phys.* **65** 1453 (1987).
2. A. B. Harris, L. I. Amstutz, H. Meyer, and S. M. Myers, *Phys. Rev.* **175**, 603 (1968).
3. F. N. H. Robinson, *J. Sci. Instr.* **36**, 481 (1959).
4. L. I. Amstutz, J. R. Thompson, and H. Meyer, *Phys. Rev. Lett.* **21**, 1175 (1968).
5. D. Ramm, *Pressure Studies in Solid* H_2 *and* D_2, *PhD thesis*, Duke University (1969) (unpubl.)
6. H. Meyer, *Phys. Rev.* **187**, 1173 (1969).
7. H. Miyagi, *Prog. Theor. Phys. (Kyoto)* **40**, 1448 (1968), A. B. Harris, *Unpublished calculations* (1968).
8. S. A. Boggs and H. L. Welsh, *Can. J. Phys.* **51**, 1910 (1973).
9. B. J. Roffey, S. A. Boggs, and H. L. Welsh, *Can. J. Phys.* **52**, 2451 (1974).
10. W. N. Hardy, A. J. Berlinsky, and A. B. Harris, *Can. J. Phys.* **55**, 1150 (1977).
11. R. Oyarzun and J. van Kranendonk, *Can. J. Phys.* **50**, 1494 (1972).
12. D. Ramm and H. Meyer, *J. Low Temp. Phys.* **40**, 173 (1980).
13. S. Washburn, R. Schweizer, and H. Meyer, *J. Low Temp. Phys.* **40**, 187 (1980).
14. I. Ya. Minchina, M. I. Bagatskii, V. G. Manzhelii, and A. I. Krivchikov, *Fiz. Nizk. Temp.* **10**, 1051 (1984) [*Sov. J. Low Temp. Phys.* **10**, 549 (1984)].
15. J. van Kranendonk, *Solid Hydrogen*, Plenum Press, New York (1983).
16. M. I. Bagatskii, A. I. Krivchikov, V. G. Manzhelii, I. Ya. Minchina, and P. I. Muromtsev, *Fiz. Nizk. Temp.* **13**, 1001 (1987) [*Sov. J. Low Temp. Phys.* **13**, 571 (1987)].
17. A. M. Meyerovich, *Private communication* (1997).
18. M. I. Bagatskii, I. Ya. Minchina, V. G. Manzhelii, and A. I. Krivchikov, *Fiz. Nizk. Temp.* **12**, 343 (1986) [*Sov. J. Low Temp. Phys.* **12**, 194 (1986)].
19. I. Ya. Minchina, M. I. Bagatskii, V. G. Manzhelii, and P. I. Muromtsev, *Fiz. Nizk. Temp.* **21**, 678 (1995) [*Low Temp. Phys.* **21**, 530 (1995)], *Czech. J. Phys, Suppl. S1* **46**, 533 (1996).
20. A. I. Krivchikov, M. I. Bagatskii, V. G. Manzhelii, I. Ya. Minchina, and P. I. Muromtsev, *Fiz. Nizk. Temp.* **15**, 3 (1989) [*Sov. J. Low Temp. Phys.* **15**, 1 (1989)].
21. X. Li, D. Clarkson, and H. Meyer, *J. Low Temp. Phys.* **78**, 335 (1990).
22. D. Clarkson and H. Meyer, *Unpublished results* (1993).
23. D. Clarkson and H. Meyer, *Fiz. Nizk. Temp.* **19**, 487 (1993) [*Low Temp. Phys.* **19**, 343 (1993)].
24. B. Ya. Gorodilov, I. N. Krupski, V. G. Manzhelii, and O. A. Korolyuk, *Fiz. Nizk. Temp.* **112**, 326 (1986) [*Sov. J. Low Temp. Phys.* **12**, 186 (1986)].
25. V. B. Kokshenev, *J. Low Temp. Phys.* **20**, 373 (1975).
26. M. Calkins and H. Meyer, *J. Low Temp. Phys.* **57**, 265 (1984).

27. J. M. Delrieu and N. S. Sullivan, *Phys. Rev.* **B23**, 3197 (1981).
28. A. E. Meyerovich, *Phys. Rev.* **B42**, 6068 (1990).
29. A. E. Meyerovich, M. P. Nightingale, and M. Tammaro, *Physica* **B194–196**, 925 (1994).
30. M. Tammaro, M. P. Nightingale, and A. E. Meyerovich, *Phys. Rev.* **B47**, 2573 (1993).
31. R. Schweizer, S. Washburn, and H. Meyer, *Phys. Rev. Lett.* **40**, 1035 (1978).
32. D. Zhou, M. Rall, J. P. Brison, and N. S. Sullivan, *Phys. Rev.* **B42**, 1929 (1990).
33. E. G. Kisvarsanyi, K. Runge, and N. S. Sullivan, *Phys. Lett.* **155A**, 337 (1991).
34. M. Rall, D. Zhou, E. G. Kisvarsanyi, and N. S. Sullivan, *Phys. Rev.* **B45**, 2800 (1992).
35. E. G. Kisvarsanyi and N. S. Sullivan, *Phys. Rev.* **B46**, 2814 (1992).
36. R. F. Buzerak, M. Chan, and H. Meyer, *J. Low Temp. Phys.* **28**, 415 (1977).
37. S. Washburn, R. Schweizer, and H. Meyer, *J. Low Temp. Phys.* **45**, 167 (1981).
38. I. Yu, *J. Low Temp. Phys.* **60**, 425 (1985).
39. N. S. Sullivan and E. Kisvarsanyi, *Private communication* (1997).
40. V. Shevtsov, A. Scherbakov, P. Malmi, E. Ylinen, and M. Punkkinen, *J. Low Temp. Phys.* **104**, 211 (1996).
41. T. Miyazaki, *Radiation Physics and Chemistry* **37**, 635 (1991).
42. K. Lee, T. Miyazaki, K. Fueki, and K. Gotoh, *J. Chem. Phys.* **10**, 341 (1987).
43. T. Miyazaki, T. Kumada, N. Kitagawa, K. Komaguchi, and Y. Aratono, *Proc. 2nd Conf. Cryocrystals 1997*, Polanica, Poland, *J. Low Temp. Phys.* **111**, 000 (1998).
44. T. Kumada, K. Komaguchi, Y. Aratono, and T. Miyazaki, *Chem. Phys. Lett.* **261**, 463 (1996).
45. T. Kumada, N. Kitasgawa, T. Takayanagi, Y. Aratono, and T. Miyazaki, *Proc. Meeting on Tunneling Reaction and Low Temperature Chemistry*, Oct 1997, JAERI, Tokai, Japan.
46. H. Meyer, *Physica* **B197**, 13 (1994).
47. L. I. Amstutz, H. Meyer, S. M. Myers, and D. C. Rorer, *Phys. Rev.* **181**, 589 (1969).
48. K. Eschenroeder, H. Kiefhaber, G. Weiss, and J. Classen, *J. Low Temp. Phys.* **109**, 163 (1997).
49. K. G. Sukhatme, J. E. Rutledge, and P. Taborek, *J. Low Temp. Phys.* **103**, 301 (1996).
50. M. Wagner and D. M. Ceperley, *J. Low Temp. Phys.* **102**, 301 (1996).
51. R. N. Conradt, U. Albrecht, S. Hermingshaus, and P. Leiderer, *Physica* **B194–196**, 679 (1994).